Eur. Phys. J. C (2014) 74:3203
DOI 10.1140/epjc/s10052-014-3203-x

THE EUROPEAN PHYSICAL JOURNAL C

Regular Article - Theoretical Physics

Double Higgs production in the littlest Higgs model with T-parity at high energy e^+e^- colliders

Bingfang Yang[1,2,a], **Zhiyong Liu**[1], **Ning Liu**[1], **Jinzhong Han**[3]

[1] College of Physics and Electronic Engineering, Henan Normal University, Xinxiang 453007, China
[2] School of Materials Science and Engineering, Henan Polytechnic University, Jiaozuo 454000, China
[3] Department of Physics and Electronic Engineering, Zhoukou Normal University, Zhoukou 466001, Henan, China

Received: 19 August 2014 / Accepted: 27 November 2014 / Published online: 11 December 2014

Abstract In the framework of the littlest Higgs model with T-parity (LHT), we investigate the double Higgs production processes $e^+e^- \to ZHH$ and $e^+e^- \to \nu\bar{\nu}HH$ at high energy e^+e^- colliders. We calculate the production cross sections and find that the relative correction at the center-of-mass energy $\sqrt{s} = 500$ GeV can maximally reach $-30\,\%$ for the process $e^+e^- \to ZHH$ and $-16\,\%$ for the process $e^+e^- \to \nu\bar{\nu}HH$ in the allowed parameter space, respectively. These large relative corrections can reach the detection range of the future e^+e^- colliders so that they can be used to test the LHT effect. The two relevant decay modes $e^+e^- \to ZHH \to l\bar{l}b\bar{b}b\bar{b}$ and $e^+e^- \to \nu\bar{\nu}HH \to \nu\bar{\nu}b\bar{b}b\bar{b}$ are studied and some distributions of the signal and background are displayed.

1 Introduction

On the 4th of July 2012, ATLAS [1] and CMS [2] collaborations have announced the existence of a Higgs-like resonance around 125 GeV confirming the cornerstone of the Higgs mechanism [3–6] that predicted such particle long times ago. However, the discovery of a Higgs-like boson is not enough to fully understand the mechanism of electroweak symmetry breaking (EWSB) and mass generation. The Higgs self-coupling is the key ingredient of the Higgs potential and its measurement is probably the most decisive test of the EWSB mechanism. To uniquely establish the Higgs mechanism experimentally, the Higgs potential of the Standard Model (SM) [7–9] must be reconstructed. In order to accomplish this, not only the Yukawa couplings and the Higgs–gauge couplings but also the Higgs self-couplings which include the trilinear coupling and the quartic coupling should be measured.

The investigation of the Higgs self-couplings requires final states containing two or more Higgs bosons. In fact, the cross sections for three Higgs boson production processes are reduced by three orders of magnitude compared to those for the double Higgs boson production [10–18], the quartic Higgs self-coupling remains elusive. The phenomenology calculations show that it is difficult to measure the trilinear Higgs self-coupling at the large Hadron collider (LHC) due to the large QCD background [19]. But the e^+e^- linear colliders, such as the international linear collider (ILC) [20] and the compact linear collider (CLIC) [21], have a clean environment and provide a possible opportunity for studying the trilinear Higgs self-coupling [10–14].

The littlest Higgs model with T-parity (LHT) [22–25] was proposed as a possible solution to the hierarchy problem and so far remains a popular candidate of new physics. At the high energy e^+e^- colliders, there are two main processes for the SM Higgs boson, $e^+e^- \to ZHH$ and $e^+e^- \to \nu\bar{\nu}HH$, where the former reaches its cross-section maximum at a center-of-mass energy of around 500 GeV, while the cross section for the latter is dominating above 1 TeV and increases towards higher energies. In the LHT model, some new particles are predicted and some couplings of the Higgs boson are modified. These new effects will alter the property of the SM Higgs boson and influence various SM Higgs boson processes, where the double Higgs production processes can provide a good opportunity to discriminate between the product group and simple group little Higgs models [26]. The single Higgs production processes in the LHT model have been investigated in our previous work [27]. In this work, we will study the double Higgs production processes, $e^+e^- \to ZHH$ and $e^+e^- \to \nu\bar{\nu}HH$.

The paper is organized as follows. In Sect. 2 we give a brief review of the LHT model related to our work. In Sect. 3 we study the effects of the LHT model in the double Higgs boson productions and present some distributions of the sig-

[a] e-mail: yangbingfang@gmail.com

nal and background. Finally, we give a short summary in Sect. 4.

2 A brief review of the LHT model

The LHT is a nonlinear σ model with a global symmetry under the $SU(5)$ group and a gauged subgroup $[SU(2) \otimes U(1)]^2$. The $SU(5)$ global symmetry is broken down to $SO(5)$ by the vacuum expectation value (VEV) of the σ field, Σ_0, given by

$$\Sigma_0 = \langle \Sigma \rangle \begin{pmatrix} \mathbf{0}_{2\times 2} & 0 & \mathbf{1}_{2\times 2} \\ 0 & 1 & 0 \\ \mathbf{1}_{2\times 2} & 0 & \mathbf{0}_{2\times 2} \end{pmatrix}. \tag{1}$$

After the global symmetry is broken, there arise 14 Goldstone bosons, which are described by the "pion" matrix Π. The Goldstone bosons are then parameterized as

$$\Sigma = \mathrm{e}^{i\Pi/f}\ \Sigma_0\ \mathrm{e}^{i\Pi^T/f} \equiv \mathrm{e}^{2i\Pi/f}\ \Sigma_0, \tag{2}$$

where f is the breaking energy scale.

The σ field kinetic Lagrangian is given by [28]

$$\mathcal{L}_\mathrm{K} = \frac{f^2}{8}\mathrm{Tr}|D_\mu \Sigma|^2, \tag{3}$$

with the $[SU(2) \otimes U(1)]^2$ covariant derivative defined by

$$D_\mu \Sigma = \partial_\mu \Sigma - i \sum_{j=1}^{2} [g_j W_{j\,\mu}^a (Q_j^a \Sigma + \Sigma Q_j^{a\,T}) + g_j' B_{j\,\mu} (Y_j \Sigma + \Sigma Y_j^T)], \tag{4}$$

where $W_j^\mu = \sum_{a=1}^{3} W_j^{\mu\,a} Q_j^a$ and $B_j^\mu = B_j^\mu Y_j$ are the heavy $SU(2)$ and $U(1)$ gauge bosons, with Q_j^a and Y_j the gauge generators, g_j and g_j' are the respective gauge couplings. In the gauge boson sector, T-parity is introduced as an exchange symmetry between the gauge bosons of the two different copies of the SM gauge group as

$$W_{1\mu}^a \longleftrightarrow W_{2\mu}^a, \quad B_{1\mu} \longleftrightarrow B_{2\mu}. \tag{5}$$

The light (L) and heavy (H) gauge fields can be obtained as

$$\begin{aligned} W_\mathrm{L}^a &= \frac{W_1^a + W_2^a}{\sqrt{2}}, \quad B_\mathrm{L} = \frac{B_1 + B_2}{\sqrt{2}}, \\ W_\mathrm{H}^a &= \frac{W_1^a - W_2^a}{\sqrt{2}}, \quad B_\mathrm{H} = \frac{B_1 - B_2}{\sqrt{2}}. \end{aligned} \tag{6}$$

The electroweak symmetry breaking $SU(2)_L \times U(1)_Y \to U(1)_{em}$ takes place via the usual Higgs mechanism. The mass eigenstates of the gauge fields are given by

$$\begin{aligned} W_\mathrm{L}^\pm &= \frac{W_\mathrm{L}^1 \mp i W_\mathrm{L}^2}{\sqrt{2}}, \\ \begin{pmatrix} A_\mathrm{L} \\ Z_\mathrm{L} \end{pmatrix} &= \begin{pmatrix} \cos\theta_\mathrm{W} & \sin\theta_\mathrm{W} \\ -\sin\theta_\mathrm{W} & \cos\theta_\mathrm{W} \end{pmatrix} \begin{pmatrix} B_\mathrm{L} \\ W_\mathrm{L}^3 \end{pmatrix}, \\ W_\mathrm{H}^\pm &= \frac{W_\mathrm{H}^1 \mp i W_\mathrm{H}^2}{\sqrt{2}}, \\ \begin{pmatrix} A_\mathrm{H} \\ Z_\mathrm{H} \end{pmatrix} &= \begin{pmatrix} \cos\theta_\mathrm{H} & -\sin\theta_\mathrm{H} \\ \sin\theta_\mathrm{H} & \cos\theta_\mathrm{H} \end{pmatrix} \begin{pmatrix} B_\mathrm{H} \\ W_\mathrm{H}^3 \end{pmatrix}, \end{aligned} \tag{7}$$

where θ_W is the usual Weinberg angle and θ_H is the mixing angle defined by

$$\sin\theta_\mathrm{H} \simeq \frac{5gg'}{4(5g^2 - g'^2)} \frac{v_\mathrm{SM}^2}{f^2}. \tag{8}$$

At $\mathcal{O}(v^2/f^2)$ in the expansion of the Lagrangian (3), the mass spectrum of the gauge bosons after EWSB is given by

$$\begin{aligned} M_{W_\mathrm{L}} &= \frac{gv}{2}\left(1 - \frac{v^2}{12f^2}\right), \\ M_{Z_\mathrm{L}} &= \frac{gv}{2\cos\theta_\mathrm{W}}\left(1 - \frac{v^2}{12f^2}\right), \quad M_{A_\mathrm{L}} = 0, \end{aligned} \tag{9}$$

$$\begin{aligned} M_{W_\mathrm{H}} &= M_{Z_\mathrm{H}} = gf\left(1 - \frac{v^2}{8f^2}\right), \\ M_{A_\mathrm{H}} &= \frac{g'f}{\sqrt{5}}\left(1 - \frac{5v^2}{8f^2}\right), \end{aligned} \tag{10}$$

where $v = v_\mathrm{SM}\left(1 + \frac{1}{12}\frac{v_\mathrm{SM}^2}{f^2}\right)$ and $v_\mathrm{SM} = 246$ GeV is the SM Higgs VEV.

The global symmetries prevent the appearance of a potential for the scalar fields at tree level. The gauge and Yukawa interactions that break the global $SO(5)$ symmetry induce radiatively a Coleman–Weinberg potential [29], V_CW, whose explicit form can be obtained after expanding the Σ field,

$$V_\mathrm{CW} = \lambda_{\phi^2} f^2 \mathrm{Tr}|\phi|^2 + i\lambda_{H\phi H} f (H\phi^\dagger H^T - H^*\phi H^\dagger) - \mu^2 |H|^2 + \lambda_{H^4}|H|^4, \tag{11}$$

where $\lambda_{\phi^2}, \lambda_{H\phi H}$ and λ_{H^4} depend on the fundamental parameters of the model, whereas μ^2, which receives logarithmic divergent contributions at one-loop level and quadratically divergent contributions at the two-loop level, is treated as a free parameter.

The HZZ, HWW and $HHZZ$, $HHWW$ couplings involved in our calculations are modified at $\mathcal{O}(v^2/f^2)$, which are given by

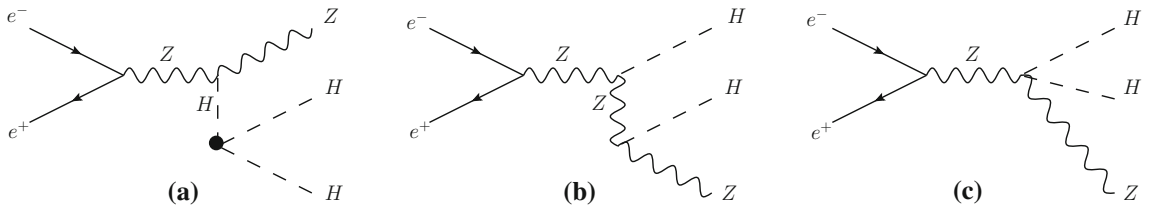

Fig. 1 Feynman diagrams for $e^+e^- \to ZHH$ at the tree level

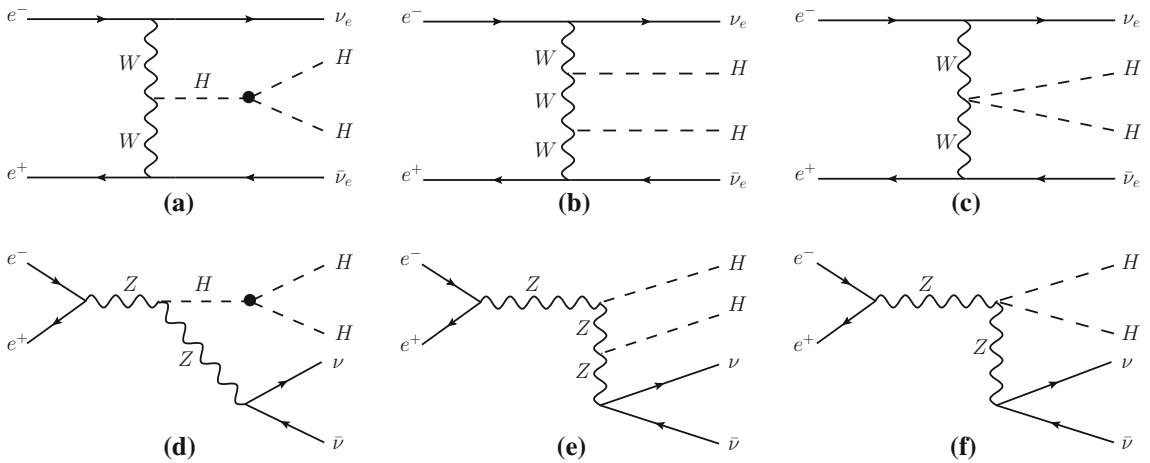

Fig. 2 Feynman diagrams for $e^+e^- \to \nu\bar{\nu}HH$ at the tree level

$$V_{HZ_\mu Z_\nu} = \frac{e^2 v}{6\cos^2\theta_W \sin^2\theta_W}\left(3 - \frac{v^2}{f^2}\right) g_{\mu\nu}, \tag{12}$$

$$V_{HW_\mu W_\nu} = \frac{e^2 v}{6\sin^2\theta_W}\left(3 - \frac{v^2}{f^2}\right) g_{\mu\nu}, \tag{13}$$

$$V_{HHZ_\mu Z_\nu} = \frac{e^2}{2\cos^2\theta_W \sin^2\theta_W}\left(1 - \frac{v^2}{f^2}\right) g_{\mu\nu}, \tag{14}$$

$$V_{HHW_\mu W_\nu} = \frac{e^2}{2\sin^2\theta_W}\left(1 - \frac{v^2}{f^2}\right) g_{\mu\nu}. \tag{15}$$

3 Calculation and numerical results

In our numerical calculations, the SM parameters are taken as follows [30]:

$$G_F = 1.16637 \times 10^{-5}\,\text{GeV}^{-2}, \quad \sin^2\theta_W = 0.231,$$
$$\alpha_e = 1/128, \quad m_H = 125\,\text{GeV},$$
$$M_Z = 91.1876\,\text{GeV}, \quad m_b = 4.65\,\text{GeV}, \quad m_e = 0.51\,\text{MeV},$$
$$m_\mu = 105.66\,\text{MeV}.$$

According to the constraints in Refs. [31–34], we require the scale to vary in the range $500\text{GeV} \le f \le 1,500$ GeV.

At the tree level, the Feynman diagrams relevant to the process $e^+e^- \to ZHH$ and the process $e^+e^- \to \nu\bar{\nu}HH(\nu = \nu_e, \nu_\mu, \nu_\tau)$ are showed in Figs. 1 and 2, respectively. In both processes, we can see that only the first column of the diagrams, i.e. Figs. 1a, 2a and d, are the signal diagrams which involve the Higgs trilinear self-coupling vertex HHH; the other ones are irreducible background diagrams. For the process $e^+e^- \to \nu\bar{\nu}HH$, the ZZ-fusion process is equally or even more important compared with the WW-fusion process at the lower center-of-mass energy.

On the left panel of Fig. 3, we show the dependence of the production cross sections σ of the processes $e^+e^- \to ZHH$ and $e^+e^- \to \nu\bar{\nu}HH$ on the center-of-mass energy $\sqrt{s}$ for the scale $f = 700$ GeV in the LHT model and the SM, respectively. We can see that the $e^+e^- \to ZHH$ cross section decreases with increasing center-of-mass energy $\sqrt{s}$ while $e^+e^- \to \nu\bar{\nu}HH$ cross section increases. The $e^+e^- \to ZHH$ cross section has the peak value around $\sqrt{s} \sim 500$ GeV. For $\sqrt{s} \sim 1$ TeV, the two cross sections are of the same order of magnitude, with $e^+e^- \to \nu\bar{\nu}HH$ being the larger source of Higgs boson pairs for $\sqrt{s} \ge 1$ TeV. Since the $\nu\bar{\nu}HH$ production is peaked in the forward region, it is important to ensure that an efficient tagging of the $HH \to b\bar{b}b\bar{b}$, $W^+W^-W^+W^-$ decay can be achieved.

On the right panel of Fig. 3, we show the dependence of the relative corrections $\delta\sigma/\sigma$ of the processes $e^+e^- \to ZHH$ and $e^+e^- \to \nu\bar{\nu}HH$ on the scale f for the center-of-mass energy $\sqrt{s} = 500$ GeV. We can see that the relative correction $\delta\sigma/\sigma$ of this two processes are both negative and decouple at the high scale f. Considering the lower bound on the scale f from the global fit of the latest experimental data [35],

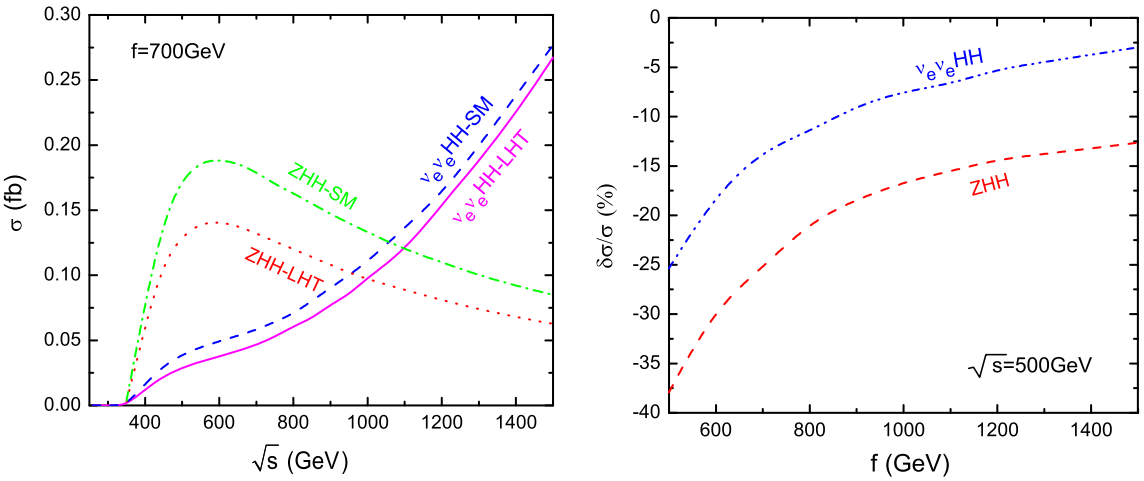

Fig. 3 The production cross sections σ versus the center-of-mass energy $\sqrt{s}$ for $f = 700$ GeV (*left*) and the relative corrections $\delta\sigma/\sigma$ versus the scale f for $\sqrt{s} = 500$ GeV (*right*)

the relative correction $\delta\sigma/\sigma$ of the process $e^+e^- \to ZHH$ can reach -30 to $-25\,\%$ and the relative correction $\delta\sigma/\sigma$ of the process $e^+e^- \to \nu\bar{\nu}HH$ can reach -16 to $-12\,\%$ for the scale f in the range 600–700 GeV. These relative correction of the cross section are significant so that they may be observed at the future e^+e^- colliders with high integrated luminosity.

In the following calculations, we will study the process $e^+e^- \to ZHH$ through the $(l\bar{l})(b\bar{b})(b\bar{b})$ mode and process $e^+e^- \to \nu\bar{\nu}HH$ through $\nu\bar{\nu}(b\bar{b})(b\bar{b})$ mode. We generate the parton-level signal and background events with MadGraph5 [36].

3.1 $e^+e^- \to ZHH \to (l\bar{l})(b\bar{b})(b\bar{b})$

For light Higgs boson masses, the Higgs boson decays predominantly in a $b\bar{b}$ pair. The $ZHH \to q\bar{q}b\bar{b}b\bar{b}$ final state benefits from a high statistics with $\sim 35\,\%$ of the final states but requires a more complicated analysis. By contrast, though $ZHH \to l\bar{l}b\bar{b}b\bar{b}(l = e, \mu)$ represents only $\sim 5\,\%$ of the total final state, this topology produces an easy signature. Therefore, we choose the $l\bar{l}b\bar{b}b\bar{b}$ final state and display some normalized distributions in the LHT model. The experimental signature is very clean, namely four b-jets (two pairs with invariant Higgs mass) plus $l\bar{l}$ with invariant Z mass.

In Fig. 4 we display the invariant mass of four b-jets M_{HH} in the SM and LHT model. The M_{HH} distribution is well known to be sensitive to the Higgs boson self-coupling, in particular for small values of the Higgs-pair mass. Since it is impossible to know which b-jet has to be paired with which $\bar{b}$-jet when reconstructing the Higgs bosons in the event, here we give the four b-jets invariant mass distribution M_{HH}.

The background events mainly come from $e^+e^- \to ZZZ \to (l\bar{l})(b\bar{b})(b\bar{b})$ and $e^+e^- \to ZZH \to (l\bar{l})(b\bar{b})(b\bar{b})$.

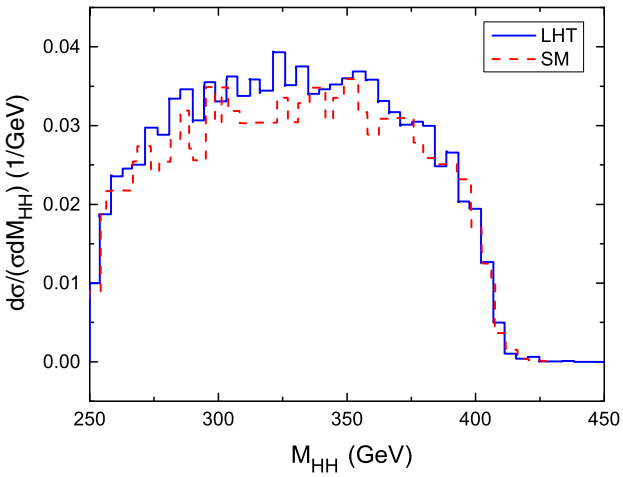

Fig. 4 Normalized M_{HH} distributions in the SM and the LHT through the production of $e^+e^- \to ZHH \to l\bar{l}b\bar{b}b\bar{b}$ for $\sqrt{s} = 500$ GeV, $f = 700$ GeV

In Fig. 5, we display the total transverse energy H_T and the transverse momentum p_T^l distributions of $(l\bar{l})(b\bar{b})(b\bar{b})$ in the signal with $f = 700$ GeV and backgrounds for $\sqrt{s} = 500$ GeV. According to Fig. 5, we can impose the cut $H_T < 450$ GeV to suppress the backgrounds. However, due to such the same parton-level final states as the signal, we need more complicated technique and more careful analysis to distinguish the signal and the backgrounds.

3.2 $e^+e^- \to \nu\bar{\nu}HH \to \nu\bar{\nu}(b\bar{b})(b\bar{b})$

Due to the dominant decay mode of Higgs is $H \to b\bar{b}$, the experimental signature for $e^+e^- \to \nu\bar{\nu}HH$ is then four b-jets (two pairs with invariant Higgs mass) plus missing energy and momentum. The dominant background $\nu\nu bbbb$ mainly

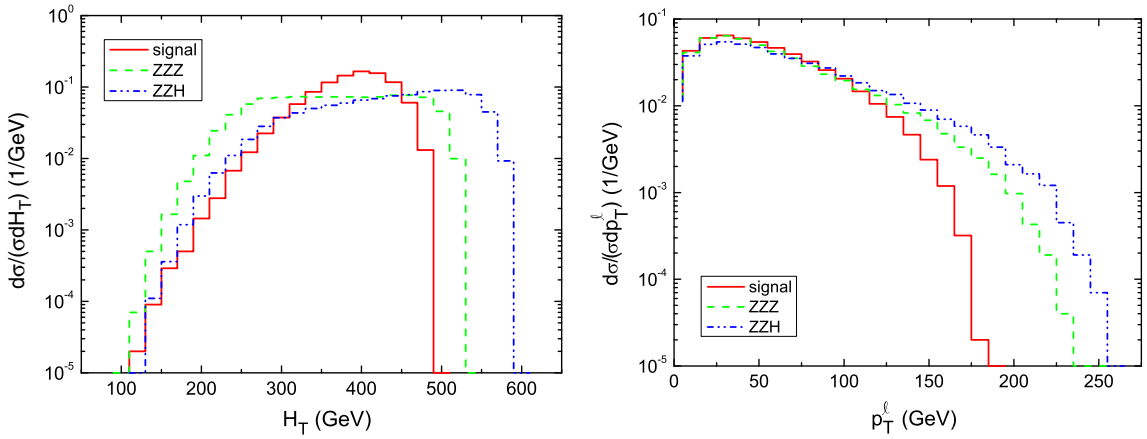

Fig. 5 Normalized distributions of H_T and p_T^l in the signal with $f = 700$ GeV and backgrounds for $\sqrt{s} = 500$ GeV

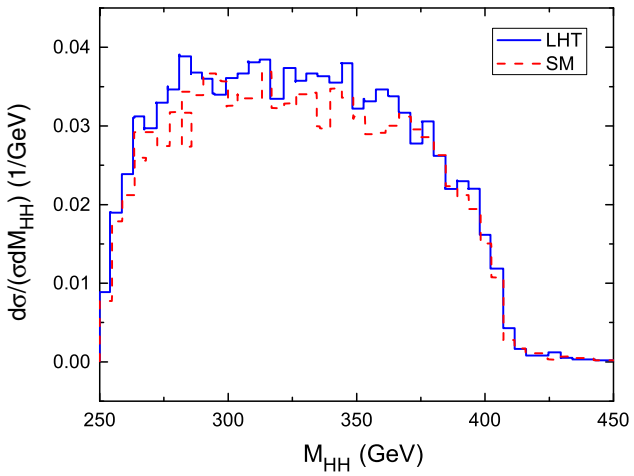

Fig. 6 Normalized M_{HH} distributions in the SM and the LHT through the production of $e^+e^- \to \nu\bar{\nu}HH \to \nu\bar{\nu}b\bar{b}b\bar{b}$ for $\sqrt{s} = 500$ GeV, $f = 700$ GeV

comes from $e^+e^- \to ZZZ$ and ZZH. Likewise, we display the invariant mass distribution M_{HH} of the four b-jets in Fig. 6.

In Fig. 7, we display the total transverse energy H_T and the missing energy $\not{E}_T$ distributions of $\nu\bar{\nu}b\bar{b}b\bar{b}$ in the signal with $f = 700$ GeV and backgrounds for $\sqrt{s} = 500$ GeV. According to Fig. 7, we can impose the cut $H_T > 300$ GeV to suppress the backgrounds.

4 Summary

In this paper, we studied the double Higgs boson productions at high energy e^+e^- colliders in the LHT model. The two main production channels $e^+e^- \to ZHH$ and $e^+e^- \to \nu\bar{\nu}HH$ have been investigated. For $\sqrt{s} = 500$ GeV, we calculated the production cross section and found that the relative correction of the process $e^+e^- \to ZHH$ can reach $-30\,\%$ and the relative correction $\delta\sigma/\sigma$ of the process $e^+e^- \to \nu\bar{\nu}HH$ can reach $-16\,\%$ when the scale f is chosen as low as 600 GeV. This result may be a probe of the LHT model at the future high energy e^+e^- colliders. In order to investigate the observability, the decay modes $e^+e^- \to ZHH \to l\bar{l}b\bar{b}b\bar{b}$ and $e^+e^- \to \nu\bar{\nu}HH \to \nu\bar{\nu}b\bar{b}b\bar{b}$ were

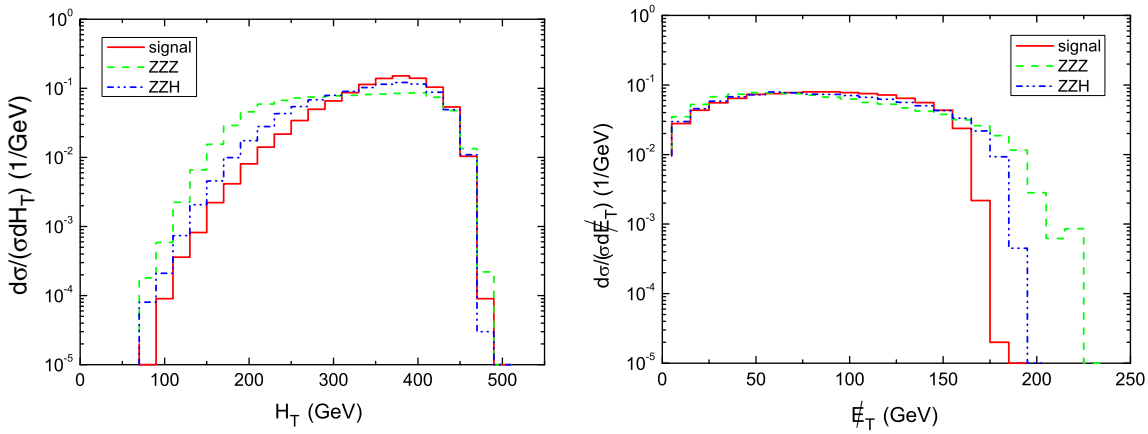

Fig. 7 Normalized distributions of H_T and $\not{E}_T$ in the signal with $f = 700$ GeV and backgrounds for $\sqrt{s} = 500$ GeV

studied and some distributions of the signal and background were presented. Due to there is only slight difference between the signals and backgrounds, more complicated technique and more careful analysis are needed to distinguish them.

Acknowledgments This work is supported by the National Natural Science Foundation of China under Grant Nos. 11405047, 11305049 and 11347140, by and the China Postdoctoral Science Foundation under Grant No. 2014M561987 and the Joint Funds of the National Natural Science Foundation of China (U1404113).

References

1. G. Aad et al., ATLAS Collaboration, Phys. Lett. B **716**, 1 (2012)
2. S. Chatrchyan et al., CMS Collaboration, Phys. Lett. B **716**, 30 (2012)
3. P.W. Higgs,Phys. Rev. Lett. **12**, 132 (1964)
4. P.W. Higgs, Phys. Rev. **145**, 1156 (1966)
5. F. Englert, R. Brout, Phys. Rev. Lett. **13**, 321 (1964)
6. G.S. Guralnik, C.R. Hagen, T.W. Kibble, Phys. Rev. Lett. **13**, 585 (1964)
7. S. Glashow, Nucl. Phys. **20**, 579 (1961)
8. A. Salam, in Elementary Particle Theory, ed. by N. Svartholm (1968)
9. S. Weinberg, Phys. Rev. Lett. **19**, 1264 (1967)
10. A. Djouadi, W. Kilian, M. Muhlleitner, P.M. Zerwas, Eur. Phys. J. C **10**, 45 (1999)
11. M. Battaglia, E. Boos, W. M. Yao, arXiv:hep-ph/0111276
12. A. Djouadi, W. Kilian, M. Muhlleitner, P.M. Zerwas, arXiv:hep-ph/0001169
13. J. Tian, K. Fujii, Y. Gao, arXiv:1008.0921 [hep-ex]
14. J. Tian, LC-REP-2013-003, http://www-flc.desy.de/lcnotes/notes/LC-REP-2013-003.pdf
15. D.A. Dicus, C. Kao, S.S. Willenbrock, Phys. Lett. B **203**, 457 (1988)
16. E.W. Glover, J.J. van der Bij, Nucl. Phys. B **309**, 282 (1988)
17. T. Plehn, M. Spira, P.M. Zerwas, Nucl. Phys. B **479**, 46 (1996)
18. T. Plehn, M. Spira, P.M. Zerwas,Erratum-ibid. B **531**, 655 (1998)
19. U. Baur, T. Plehn, D. Rainwater, Phys. Rev. Lett. **89**, 151801 (2002)
20. T. Behnke, J.E. Brau, B. Foster et al., arXiv:1306.6327 [physics.acc-ph]
21. P. Lebrun, L. Linssen, A. Lucaci-Timoce et al., arXiv:1209.2543 [physics.ins-det]
22. H.C. Cheng, I. Low, JHEP **0309**, 051 (2003)
23. H.C. Cheng, I. Low, JHEP **0408**, 061 (2004)
24. I. Low, JHEP **0410**, 067 (2004)
25. J. Hubisz, P. Meade, Phys. Rev. D **71**, 035016 (2005)
26. W. Kilian, D. Rainwater, J. Reuter, Phys. Rev. D **74**, 095003 (2006)
27. B. Yang, J. Han, S. Zhou, N. Liu, J. Phys. G Nucl. Part. Phys. **41**, 075009 (2014)
28. N. Arkani-Hamed, A.G. Cohen, E. Katz, A.E. Nelson, JHEP **0207**, 034 (2002). arXiv:hep-ph/0206021
29. S.R. Coleman, E.J. Weinberg, Radiative corrections as the origin of spontaneous symmetry breaking. Phys. Rev. D **7**, 1888C1910 (1973)
30. J. Beringer et al., Particle Data Group, Phys. Rev. D **86**, 010001 (2012)
31. J. Hubisz, P. Meade, A. Noble, M. Perelstein, JHEP **0601**, 135 (2006)
32. B. Yang, X. Wang, J. Han, Nucl. Phys. B **847**, 1 (2011)
33. J. Reuter, M. Tonini, JHEP **0213**, 077 (2013)
34. J. Reuter, M. Tonini, M. de Vries, arXiv:1307.5010 [hep-ph]
35. B. Yang, G. Mi, N. Liu, JHEP **10**, 047 (2014). arXiv:1407.6123 [hep-ph]
36. J. Alwall et al., JHEP **1106**, 128 (2011)